Ti-Based Catalysts on Magnesium Hydride

Subjects: Chemistry, Inorganic & Nuclear

Contributor: Chengshang Zhou

Magnesium-based hydrides are considered as promising candidates for solid-state hydrogen storage and thermal energy storage, due to their high hydrogen capacity, reversibility, and elemental abundance of Mg. To improve the sluggish kinetics of MgH2, catalytic doping using Ti-based catalysts is regarded as an effective approach to enhance Mg-based materials.

Keywords: magnesium hydride ; titanium-based hydride ; catalysis ; hydrogen storage properties

1. Introduction

Depletion of fossil fuels and changes in the global climate urge people to seek green, sustainable energy resources and high-efficiency energy systems. Hydrogen is one of the secondary energy solutions with high gravimetric energy density, high efficiency, and zero carbon emission [1]. However, the hydrogen economy relies on safe and mature technology to store hydrogen, which remains a great challenge [2]. Solid-state hydrogen storage using metal hydrides is considered to be a safe and efficient method in comparison to other storage technologies, such as compressed hydrogen gas or liquid hydrogen.

Among various solid-state hydrogen storage materials, magnesium hydride (MgH_2) is one of the metal hydrides that has been considered to be promising, due to its high storage capacity, abundant resources, and relative safety. MgH_2 was first prepared in 1912 [3], and was proposed that can be used as energy storage media since the 1960s [4]. MgH_2 is known for its high hydrogen storage content, up to 7.76 wt%. More importantly, Mg has a single and flat pressure plateau under desorption/absorption, and is an abundant resource in the crust, which makes it one of the most promising hydrogen storage materials comparing to others. Thus, Mg-based hydride is expected to play important roles in future hydrogen storage techniques. In past decades, research efforts have made significant progress on improving Mg-based hydrides in terms of thermodynamics, kinetics, and reversibility. The utilization of MgH_2 for “energy storage” relates to two aspects, namely, hydrogen storage (HS) [5] and thermal energy storage (TES) [6]. Despite the difference in material-level for HS and TES, both applications require Mg-based hydride with fast hydrogen absorption and desorption rates. This leads to a large demand for studying catalysis in the Mg-H_2 system.

Due to the extensive research activities on Mg-based hydrides, a series of review papers have been published [7][8][9][10][11][12][13][14]. A comprehensive review by Yartys et al. [15] provides a historical overview as well as future perspectives. Recent reviews have covered various directions for Mg-based hydrogen storage, such as downsizing (nanostructuring) [7][10], catalysis and kinetics [7][16][17], and destabilization [18][19].

2. Fundamentals of the Mg-H_2 System

2.1. Crystal Structure

MgH_2 is a stoichiometric compound with a H/Mg atomic ratio of 1.99 ± 0.01 [20]. The Mg-H bond is an ionic type that is similar to alkali and alkaline earth metal hydrides [21]. MgH_2 with different types of structures can be synthesized by the reaction of magnesium with hydrogen under different conditions. β-MgH_2, which is stable at ambient pressure (1 bar) and room temperature, has a tetragonal TiO_2-rutile-type structure with space group $P4_2/mnm$ [22]. β-MgH_2 can be formed under moderate conditions during reversible hydrogen cycling. Nevertheless, MgH_2 has at least four high-pressure forms, and the corresponding crystal structure parameters are tabulated in Table 1. At high applied pressures exceeding 0.387GPa or milled under high energy, β-MgH_2 transforms into the orthorhombic γ-MgH_2 form with α-PbO_2-type structure [23]. Additionally, a subsequent phase transition from γ-MgH_2 to a modified-CaF_2-type structure was observed experimentally using in situ synchrotron diffraction when hydrogen pressure is above 3.84 GPa [24]. According to Varin et al., high energy ball-milling of MgH_2 produced γ-MgH_2 coexisted with nanocrystalline β-MgH_2. They suggested that the presence of the γ-MgH_2 phase contributed to reducing the hydrogen desorption temperature of MgH_2 [25].

Table 1. Optimized structural parameters, bulk modulus (B_0), and pressure derivative of bulk modulus (B'_0) for MgH_2 in ambient and high-pressure phases. (Reprinted with permission from ref. [22]. Copyright 2006 American Physical Society).

Modification	Unit Cell (Å)			Positional Parameters	B_0 (GPa)	B'_0
Structure Type	a	b	c			
β-MgH_2, TiO_2-rutile ($P4_2/mnm$)	4.5176	4.5176	3.0206	Mg (2*a*): 0, 0, 0	45.00 ± 2	3.35 ± 0.3
$\gamma - MgH_2$, Modified CaF_2 ($Pa\bar{3}$)	4.6655	4.6655	4.6655	Mg (4*a*): 0, 0, 0	47.41 ± 4	3.49 ± 0.4
α-MgH_2, α-PbO_2 (P_{bcn})	4.5246	5.4442	4.9285	Mg (4*c*): 0, 0.3313[d], 1/4[d]	44.03 ± 2	3.17 ± 0.4
δ'-MgH_2, $AuSn_2$ (P_{bca})	8.8069	4.6838	4.3699	Mg (8*c*): (0.8823, 0.0271, 0.2790)	49.83 ± 5	3.49 ± 0.6

2.2. Thermodynamics of the Mg-H_2 System

The first experimental evaluation of the thermodynamics of the Mg-H_2 system was reported by Stampfer et al., showing the enthalpy of formation of MgH_2 to be −74.5 kJ/mol·H_2, and the entropy of formation is 136 J/K·mol·H_2 [20]. The thermodynamics parameters of the Mg-H_2 system have been reported, see Table 2. The pressure-composition-isotherm (PCI) method is commonly used to determine the enthalpy (ΔH) and entropy (ΔS) of the Mg-H_2 system. By measuring a series of equilibrium pressures at various temperatures, ΔH and ΔS can be derived by Van't Hoff relation.

Table 2. Thermodynamic parameters and energy storage properties of MgH_2 [26].

Thermodynamic Parameters	Values
Formation enthalpy, kJ/(mol·H_2)	−74.5
Formation entropy, J/(mol·H_2·K)	−135
Hydrogen Storage Capacity (Theoretical)	
Gravimetric capacity, wt%	7.6
Volumetric capacity, g/(L·H_2)	110
Thermal Energy Storage Capacity (Theoretical)	
Gravimetric capacity, kJ/kg	2204
Volumetric capacity, kJ/dm^3	1763

For on-board solid-state hydrogen storage, a thermodynamic window in the range of approximately 25–45 kJ/mol·H_2 is recognized for suitable metal hydride material [27]. Therefore, efforts have been directed to destabilize the MgH_2, or in other words, reducing the ΔH of MgH_2. It is expected that reducing ΔH can lower the working temperature for Mg-based hydride, which is crucial for on-board applications. Three typical approaches were proposed to destabilize MgH_2, namely, alloying, downsizing, and stress effect.

The alloying method refers to alloying other elements with Mg to form a new alloy or hydride compound with lower stability of its hydride. So far, alloying systems have been reported including Mg_2NiH_4 [28], Mg_2FeH_6, Mg_2CoH_5, Mg_2Cu [29], Mg(Al) [30], $Mg_{51}Zn_{20}$ [31], Mg_2Si [32], Mg(In) [33], Mg(Sn) [21], Mg(AgIn) [34], MgReNi [35], Mg_2M-xM_xH_y (M = Fe, Co, Ni), and so on. The principle is using a less-stable hydriding element A to form an Mg-A alloy. The energy diagram of the alloying method is illustrated in Figure 1. Since Mg-Ti is an immiscible system, Mg and Ti do not form an alloy. However, metastable Mg-Ti-H compounds have been reported. Kohta et al. [36][37][38][39] successfully synthesized Mg_xTi_{100-x} ($35 \le x \le 80$) alloys with hexagonal close-packed (HCP), face-centered cubic (FCC), and body-centered cubic (BCC) structures by ball milling. Vermeulen et al. [40] reported that Mg-Ti-H system has a very low plateau pressure (≈10^{-6} bar at room temperature). Additionally, it will have a higher plateau pressure and a reversible hydrogen storage capacity of more than 6 wt%, when forming ternary compositions with Al or Si.

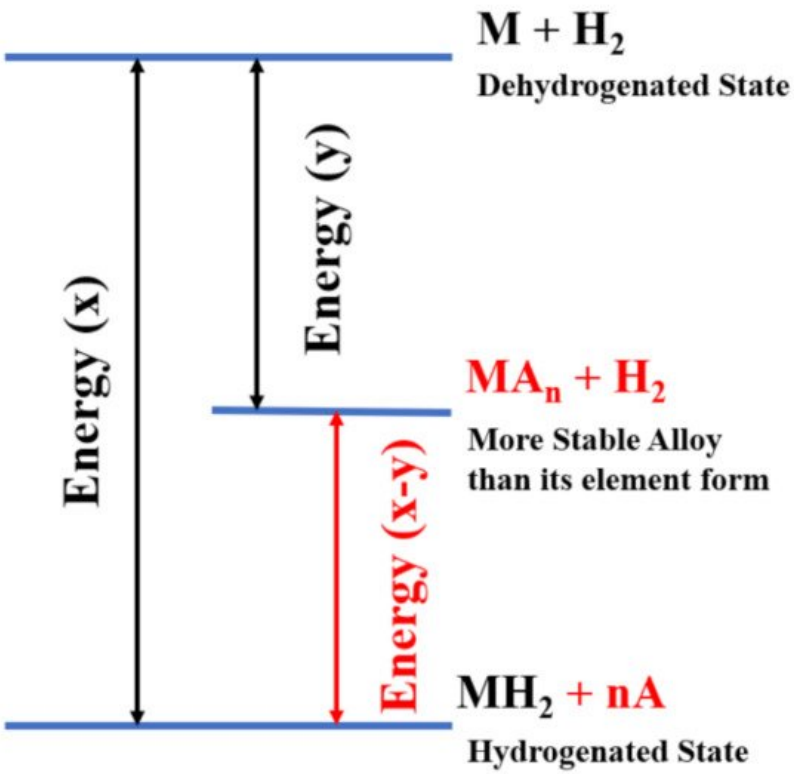

Figure 1. Schematic of destabilization process of a hydride MH using third element A. (Reproduced with permission from ref. [41]. Copyright 2016 Elsevier).

Nano-sizing of Mg-based materials is not only a strategy to enhance kinetics, but also considered as an approach to destabilize MgH_2. It has attracted a great deal of effort in the past decades, despite its effectiveness and feasibility remaining controversial. The influence of nano-sizing on pressure-temperature dependence as well as ΔH is given in Figure 2. Theoretically, nanosizing to hydrides introduces excessive free energy to bulk or coarse particles. The excessive free energy may originate from lattice distortion [42]. Sadhasivam et al. [8] summarized the dimensional effects of nanostructured Mg/MgH_2 materials. They reported that Mg/MgH_2 with a particle size <5 nm has improved hydrogen storage properties. However, a great challenge remains in synthesizing such fine particles as well as maintaining the nano-size after thermal cycling for Mg-based materials. According to [8], the 1-dimensional Mg nanowire shows a promising hydrogen storage property. However, the nanowire structure would collapse into nanoparticles after a few cycles. Additionally, it is reported that reducing magnesium hydride structure to nanosize induces the stress/strain effect, which has been reviewed by Zhang et al. [43] It was pointed out that the stress/strain applied on MgH_2 leads to lattice deformation and volume change, which endows the extra strain energy for MgH_2. The research of Berube et al. [44] supported this claim. They reported that a 15% reduction of the formation enthalpy of nanostructured MgH_2 can be achieved by the introduction of surfaces, grain boundaries, as well as the presence of γ-MgH_2. Recent reviews [8][45][46], have provided thoughtful introduction and discussion into the thermodynamic aspects.

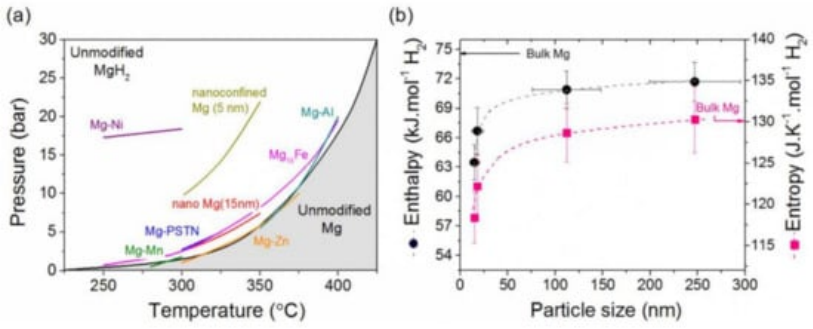

Figure 2. (**a**)Temperature dependence of the dissociation pressure of MgH_2 and associated evolution of such a dissociation pressure for various approaches investigated, and (**b**) evolution of ΔH and ΔS as a function of the particle size of Mg. (Reproduced with permission from ref. [47]. Copyright 2018 Elsevier).

2.3. Kinetics

Kinetics for hydrogen storage materials is generally defined as the dynamic rate where hydrogenation and dehydrogenation take place in time. Kinetics measurements provide critical information on the rates of hydrogen uptake or

release from Mg-based materials. It is necessary to be rather explicit when investigating hydrogenation and dehydrogenation kinetics. For pure Mg and MgH_2 in the conventional form of coarse powders, they demonstrate very sluggish kinetics for hydrogen absorption and release, usually requiring over 400 °C for the reverse reactions. The slow hydrogenation rate of Mg, as well as dehydrogenation rate of MgH_2, can be attributed to several intrinsic factors: dissociation of the hydrogen molecule, penetration of hydrogen through the surface, diffusion of hydrogen in the matrix, in addition to possible contamination in the sample environment.

For hydrogenation of Mg, dissociation of the hydrogen molecule on the Mg surface is often considered as a rate-limiting step. Table 3 summarizes the energies for hydrogen molecule dissociation on Mg and modified Mg surfaces. The reported values of hydrogen dissociation energy on the Mg surface are in the range of 0.4–1.15 eV (38.59–110.96 kJ/mol), which is higher than most transition metals, such as Ti, V, Ni, and Fe [48]. This means that a large energy barrier needs to be overcome for dissociation of H_2 on pure Mg (0001) surfaces [49]. Another intrinsic issue is the slow hydrogen diffusion rate in MgH_2. Figure 3 shows the geometry model of the reaction for an Mg/MgH_2 particle. Based on the model, the hydride layer formed on the particle surface becomes the major barrier during hydrogenation, since the hydrogen atom diffusion rate in the hydride phase is much slower than that in the metallic phase. According to Spatz et al., the hydrogen diffusion coefficient (D_H) of MgH_2 is quite low (1.1×10^{-20} m^2/s at 305 K) [50]. Figure 4 shows that the D_H of MgH_2 is at magnitudes lower than the D_H of the Mg metal phase. It is also evident in this figure from the diffusion coefficient plots that most transition metals and their hydrides have D_H several magnitudes higher than the D_H of MgH_2.

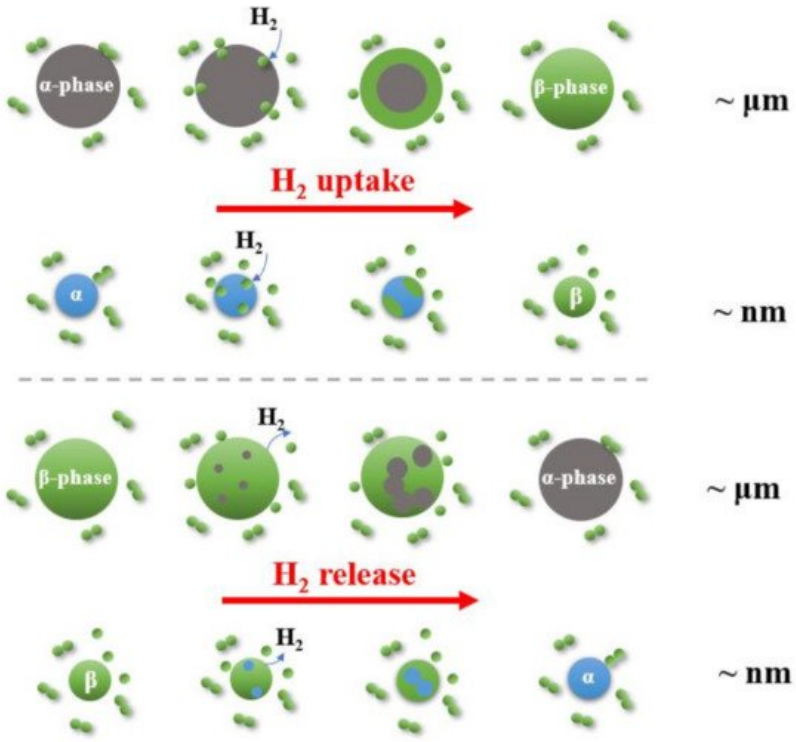

Figure 3. Schematic of the hydrogen absorption/desorption process in the MgH_2/Mg. (Reproduced with permission from ref. [47]. Copyright 2018 Elsevier).

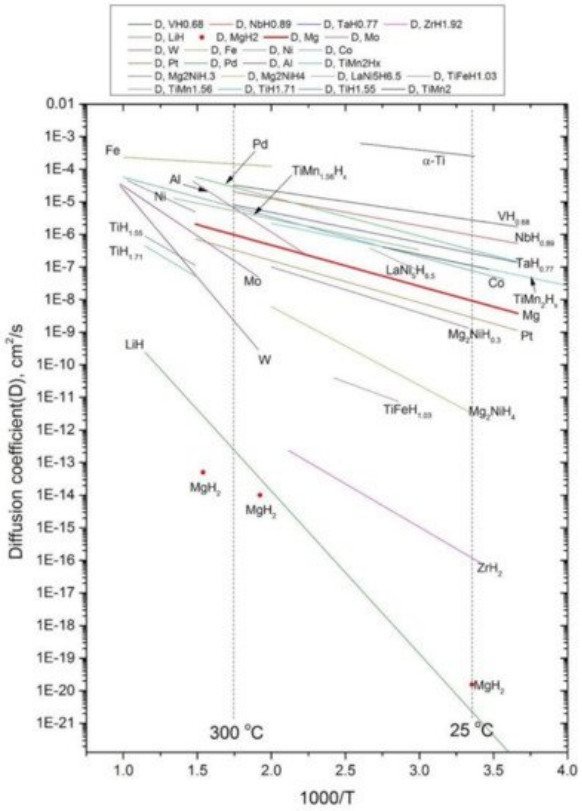

Figure 4. Hydrogen diffusion coefficients in different metals and hydrides. (Reprinted from ref. [51]. Copyright 2015 Chengshang Zhou).

Table 3. Dissociation energy of hydrogen molecule on the surface of Mg. (Reproduced with permission from ref. [49]. Copyright 2008 AIP Publishing).

Metal	Dissociation Energy (eV)
Pure Mg	0.87, 0.40, 0.50, 1.15, 1.05, 0.95, 1.00
Ti-doped Mg	Null, negligible
Ni-doped Mg	0.06
V-doped Mg	Null
Cu-doped Mg	0.56
Pd-doped Mg	0.39
Fe-doped Mg	0.03
Ag-doped Mg	1.18

Catalytic doping and nanosizing of Mg-based systems have been considered as important methods to improve their kinetics. In general, the catalyst is defined as an agent which reduces the activation barrier without participating in the chemical reaction, as illustrated in Figure 5. A common consensus is that transition metals (TM) and their compounds are effective catalysts. These catalysts can be doped into Mg/MgH_2 material by different synthetic approaches. Most TM catalysts are effective in both hydrogenation and dehydrogenation reactions. The roles of different Ti-based catalysts and the underlying mechanism will be reviewed in the following section.

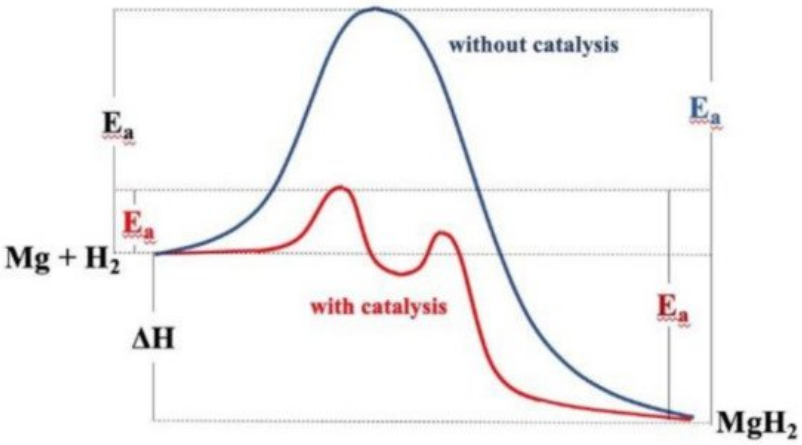

Figure 5. Representation of the kinetic barrier of the reaction and lowering the activation energy (E_a) using a catalyst. (Reprinted from ref. [52]. Copyright 2018 MDPI).

Downsizing MgH_2 to nano-scale is also shown to be effective to improve the kinetics. It is believed that nano-sizing can enhance kinetics by the creation of a large amount of fresh surface, shortening hydrogen diffusion, and promoting nucleation of the hydride/metal phase [12]. It is noteworthy that a combination of nanosizing and catalytic doping is usually realized during synthesis. For example, using a high-energy ball milling technique, co-milling MgH_2 with transition metal powder could produce a nanocomposite with nano-size microstructure and homogeneously doped catalyst particles.

3. Catalytic Effects

3.1. Transition Metals Catalysts

Among various additives for improving Mg-based materials, TM catalysts have been intensively investigated. Interestingly, most of the transition metals and their compounds are found to be effective as both hydrogenation and dehydrogenation catalysts. In general, 1–5 at.% addition of TM catalyst leads to dramatic improvement while the hydrogen storage capacity is not sacrificed significantly. Research efforts have been directed to investigate the effectiveness of various TM-based catalysts. Table 4 compiles the reported results from Ti-based additive-enhanced MgH_2 systems as well as corresponding synthetic approaches and kinetic behaviors.

Table 4. Hydrogen storage properties of Mg with various types of Ti-based catalysts.

Materials	Synthetic Methods	Hydrogen Storage Properties				Reference
		Desorption Kinetics	Ea_{des} (kJ/mol)	Absorption Kinetics	Ea_{abs} (kJ/mol)	
Titanium/Titanium Hydrides						
Mg-2%Ti	Inert gas condensation	Des: 4.50%/320 °C/0.2 bar/25 min		Abs: 4.80%/320 °C/8 bar/21 min		[53]

Materials	Synthetic Methods	Hydrogen Storage Properties				Reference
		Desorption Kinetics	Ea_{des} (kJ/mol)	Absorption Kinetics	Ea_{abs} (kJ/mol)	
Titanium/Titanium Hydrides						
MgH_2 + 2 at% Ti	Ball milling (argon)	Des: 6.32 wt%/623 K/35 kPa/0.5 h		Abs: 6.32 wt%/623 K/2000 kPa/4 min		[54]
	Cold rolling (5 times, air)	Des: 6.00 wt%/623 K/35 kPa/0.5 h		Abs: 5.70 wt%/623 K/2000 kPa/4 min		
MgH_2-4 mol% Ti	Ball milling	Des: 1.10%/573 K/2 MPa/5 min		Abs: 6.40%/573 K/2 MPa/5 min		[55]
MgH_2-5 at% Ti	Ball milling	Des Temperature: 235.6 °C	70.11			[56]
MgH_2-5 at% Ti	Ball milling	Des: 5.50%/523 K/0.015 MPa/20 min	71.1	Abs: 4.20%/373 K/1.0 MPa/15 min		[57]
MgH_2-5 at% Ti	Ball milling	Des: 5.20%/573 K/0.03 MPa/15 min		Abs: 6.70%/ 573 K/0.8 MPa/15 min		[58]
Mg-5% Ti	Chemical vapor synthesis		104			[59]
Mg-14 at% Ti	Gas phase condensation		35		52	[60]
Mg-22 at% Ti			31		47	
MgH_2-15% Ti	Ball milling	Des: 0.12%/573 K/1 bar/60 min		Abs: 3.48%/573 K/12 bar/60 min		[61]

Materials	Synthetic Methods	Hydrogen Storage Properties				Reference
		Desorption Kinetics	Ea_{des} (kJ/mol)	Absorption Kinetics	Ea_{abs} (kJ/mol)	
Titanium/Titanium Hydrides						
$Mg_{0.9}Ti_{0.1}$	Ball milling		76	Abs: 6.62% (after milling)		[62]
$Mg_{0.75}Ti_{0.25}$	Ball milling		88	Abs: 6.18% (after milling)		
$Mg_{0.5}Ti_{0.5}$	Ball milling		91	Abs: 5.21% (after milling)		
MgH_2-20% Ti	Ball milling		72 ± 3			[63]
MgH_2-coated Ti	Ball milling	Des: 5.00%/250 °C/15 min (TPD) Des Temperature: 175 °C				[64]
$Mg_{83.5}Ti_{16.5}$	Inert gas condensation	Des: 2.50%/300 °C/0.15 bar/2 min		Abs: 2.20%/300 °C/9 bar/1 min		[65]
15Mg-Ti	Chemical method				72.2	[66]
MgH_2-4 mol% TiH_2	Ball milling	Des: 0.70%/573 K/2 MPa/5 min		Abs: 6.10%/573 K/2 MPa/5 min		[55]
MgH_2-5 at% TiH_2	Ball milling	Des: 5.80%/270 °C/0.12 bar/10 min Des Temperature: 235.5 °C	67.24	Abs: 2.70%/25 °C/1 bar/250 min		[56]
10MgH_2-TiH_2	Ball milling		73			[67]
7MgH_2-TiH_2	Ball milling		71			[68]
4MgH_2-TiH_2	Ball milling		68			[68]
MgH_2-10 mol% TiH_2	Ball milling			Abs: 5.70%/240 °C/2 MPa/200 s	16.4	[69]

Materials	Synthetic Methods	Hydrogen Storage Properties				Reference
		Desorption Kinetics	Ea_{des} (kJ/mol)	Absorption Kinetics	Ea_{abs} (kJ/mol)	
Titanium/Titanium Hydrides						
MgH_2-10% TiH_2	Ball milling				24.2	[70]
MgH_2-10% TiH_2	Ball milling				17.9	[71]
Mg-9.2% $TiH_{1.971}$-3.7% $TiH_{1.5}$	Ball milling	Des: 4.10%/573 K/100 Pa/20 min	46.2	Abs: 4.30%/298 K/4 MPa/10 min	12.5	[72]
$Mg_{0.65}Ti_{0.35}D_{1.2}$	Ball milling		17			[73]
Titanium Oxides						
MgH_2-10% TiO_2	Ball milling	Des: 6.00%/300 °C/vacuum/20 min		Abs: 6.00%/300 °C/0.84 MPa/5 min		[74]
Mg-20% TiO_2	Reactive ball milling	Des: 4.40%/350 °C/1 bar/8.5 min		Abs: 3.80%/350 °C/20 bar/2 min		[75]
MgH_2-6% TiO_2	Ball milling		145.8 ± 14.2			[76]
MgH_2 + 10% TiO_2	Ball milling	Des Temperature: 200 °C	75.50			[77]
Titanium Halides						
MgH_2-10% TiF_4	Ball milling	Des Temperature: 216.7 °C	71	(Des: 6.6%)		[78]
MgH_2-10% TiF_4	Ball milling (2 h, argon)	Des Temperature: 154 °C	70			[79]
MgH_2 + 10% TiF_4	Ball milling	Des Temperature: 150 °C	70			[77]

Materials	Synthetic Methods	Hydrogen Storage Properties				Reference
		Desorption Kinetics	Ea_{des} (kJ/mol)	Absorption Kinetics	Ea_{abs} (kJ/mol)	
Titanium/Titanium Hydrides						
MgH_2-4 mol% TiF_3	Ball milling	Des: 4.50%/573 K/2 MPa/5 min		Abs: 5.10%/573 K/2 MPa/5 min		[55]
MgH_2-4 mol% $TiCl_3$	Ball milling	Des: 3.70%/573 K/2 MPa/5 min		Abs: 5.30%/573 K/2 MPa/5 min		[55]
MgH_2-7% $TiCl_3$	Ball milling	Des temperature: 274 °C	85			[80]
Titanium Alloys						
MgH_2-5a% TiAl	Ball milling	Des: 4.90%/270 °C/0.12 bar/10 min Des Temperature: 219.6 °C	65.08	Abs: 2.50%/25 °C/1 bar/250 min		[56]
MgH_2-5 a% Ti_3Al	Ball milling	Des Temperature: 232.3 °C	70.61			[56]
$Mg_{85}Al_{7.5}Ti_{7.5}$	DC-magnetron co-sputtering	Des: 5.30%/200 °C/vacuum/20 min		Abs: 5.60%/200 °C/3 bar/0.5 min		[81]
$Mg_{0.63}Ti_{0.27}Si_{0.10}D_{1.1}$	Ball milling		27			[73]
MgH_2-5 at%TiNi	Ball milling	Des Temperature: 242.4 °C	73.09			[56]
15Mg-Ti-0.75Ni	Chemical method				63.7	[66]
$Mg_{0.63}Ti_{0.27}Ni_{0.10}D_{1.3}$	Ball milling		21			[73]
MgH_2-5at%TiNb	Ball milling	Des: 5.90%/27 °C/0.12 bar/10 min Des Temperature: 231.3 °C	71.72	Abs: 2.80%/25 °C/1 bar/250 min		[56]

Materials	Synthetic Methods	Hydrogen Storage Properties				Reference
		Desorption Kinetics	Ea_{des} (kJ/mol)	Absorption Kinetics	Ea_{abs} (kJ/mol)	
Titanium/Titanium Hydrides						
MgH_2-5at% Cr-5a% Ti	Film	Des: 6.00%/200 °C/5 mbar/25 min		Abs: 6.20%/200 °C/3 bar/10 min		[82]
MgH_2-7 at% Cr-13 at% Ti	Film	Des: 5.00%/200 °C/5 mbar/25 min		Abs: 5.60%/200 °C/3 bar/10 min		
MgH_2-5 at% TiFe	Ball milling	Des: 5.20%/270 °C/0.12 bar/10 min Des Temperature: 237.7 °C	72.63	Abs: 3.00%/25 °C/1 bar/250 min		[56]
MgH_2-5% FeTi	Ball milling			Abs: 2.30%/150 °C/2 MPa/5 min	21	[83]
MgH_2-5 at% $TiMn_2$	Ball milling	Des: 4.80%/270 °C/0.12 bar/10 min Des Temperature: 219.7 °C	74.22	Abs: 3.20%/25 °C/1 bar/250 min		[56]
MgH_2-10% $TiMn_2$	Ball milling				22.6	[70]
MgH_2-5% VTi	Ball milling			Abs: 3.30%/150 °C/2 MPa/5 min	10.4	[83]
$Mg_{87.5}Ti_{9.6}V_{2.9}$	Hydrogen plasma metal reaction	Des: 4.00%/300 °C/1 mbar/5 min	73.8	Abs: 4.80%/200 °C/40 bar/5 min	29.2	[84]
MgH_2-5 at% TiVMn	Ball milling	Des: 5.70%/270 °C/0.12 bar/10 min Des Temperature: 216.7 °C	85.20	Abs: 3.00%/25 °C/1 bar/250 min		[56]
Multiple Catalysts						

Materials	Synthetic Methods	Hydrogen Storage Properties				Reference
		Desorption Kinetics	Ea_{des} (kJ/mol)	Absorption Kinetics	Ea_{abs} (kJ/mol)	
Titanium/Titanium Hydrides						
Mg-10% Ti-10% Pd	Ball milling		114 ± 4			[85]
Mg-$TiH_{1.971}$-$TiH_{1.5}$-$ZrH_{1.66}$	Arc melting		36.6		21.2	[86]
$Mg_{0.9}Ti_{0.1}$ + 5% C	Ball milling		88	Abs: 6.43% (after milling)		[62]
MgH_2-6% $NiTiO_3$	Ball milling		74 ± 4			[87]
MgH_2-6% $CoTiO_3$	Ball milling		100 ± 2			[87]
MgH_2-10 mol% TiH_2-6 mol% TiO_2	Ball milling		118			[88]
MgH_2-5% VTi-CNTs	Ball milling			Abs: 5.10%/150 °C/2 MPa/5 min	10.2	[83]
MgH_2-5% FeTi-CNTs	Ball milling			Abs: 0.60%/150 °C/2 MPa/5 min	65.5	[83]
MgH_2-10% Ni-TiO_2	Ball milling	Des: 6.50%/265 °C/0.02 bar/7 min	43.7 ± 1.5	Abs: 5.00%/100 °C/60 bar/7 min		[76]
MgH_2-4% Ni-6% TiO_2	Ball milling		91.6 ± 8.5			[76]
MgH_2-10% Co-TiO_2	Ball milling	Des: 6.20%/250 °C/0.02 bar/15 min	77	Abs: 4.24%/100 °C/60 bar/10 min		[89]

Early work by Liang et al. [57] evaluated the catalytic effects of 3d-TM elements (Ti, V, Mn, Fe, and Ni) on the reaction kinetics of ball-milled catalyzed MgH_2 (see Figure 6). The MgH_2-Ti composite showed superior hydrogen desorption/absorption kinetics, exhibiting the best desorption kinetics at 573 K, followed in order by V, Fe, Ni, and Mn. The activation energies (E_a) of MgH_2-Ti, MgH_2-V, MgH_2-Mn, MgH_2-Fe, and MgH_2-Ni are calculated to be 71.1 kJ/mol, 62.3 kJ/mol, 104.6 kJ/mol, 67.6 kJ/mol, and 88.1 kJ/mol, respectively, which are significantly reduced compared to that of the ball-milled pure MgH_2 (120 kJ/mol). It was indicated that the TM catalysts could drastically improve the kinetic properties

of MgH_2, among which Ti-catalyzed MgH_2 shows superior performance. Rizo-Acosta et al. [58] compared hydrogenation properties of MgH_2 with the addition of early transition metals (Sc, Y, Ti, Zr, V, and Nb). As shown in Figure 7a,b, their results indicated that full reactions finished within less than 120 min in all cases and the hydrogen absorption rate increased along the sequence Y < V < Ti < Nb < Sc < Zr. However, an apparent degradation was observed when the cycling number increases. Interestingly, this evolution is less pronounced in the Ti-doped system, as shown in Figure 7c, which was attributed to the lattice mismatch between Mg and TiH_2 hydride that limits Mg grain growth. Among all cases, MgH_2-TiH_2 nanocomposite presented the best cycling properties with a reversible capacity of 4.8 wt% after 20 cycles and the reaction time arbitrarily limited to 15 min.

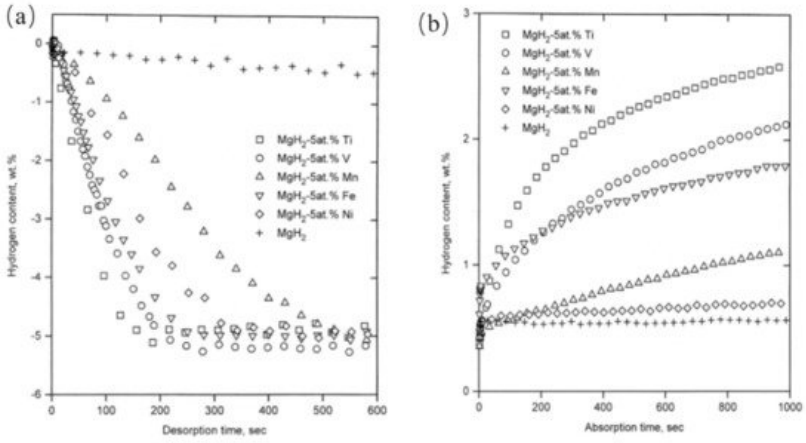

Figure 6. Hydrogen desorption curves ((**a**), desorption pressure of 0.015 MPa, 573 K) and absorption curves ((**b**), absorption pressure is 1.0 MPa, 302 K) of Mg–Tm composites. (Reproduced with permission from ref. [57]. Copyright 1999 Elsevier).

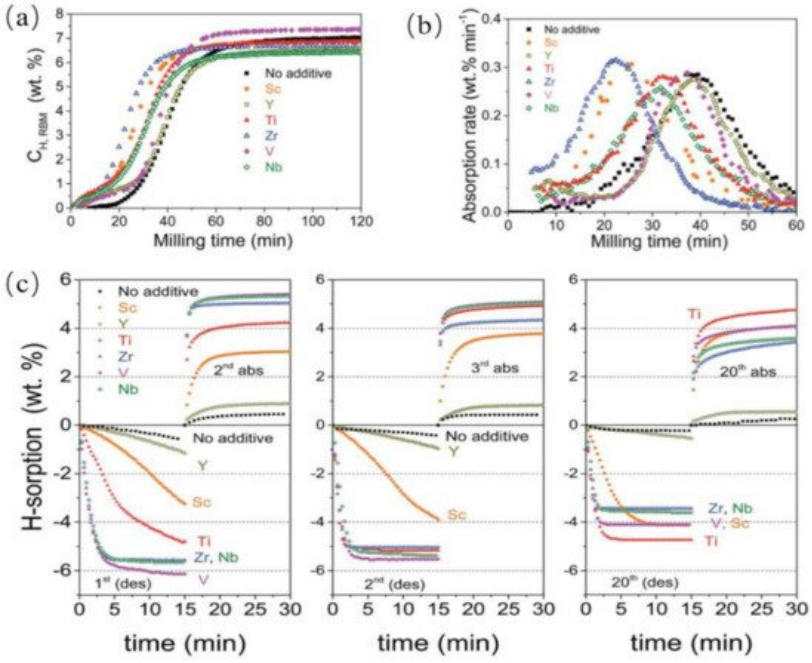

Figure 7. (**a**) Hydrogen uptake curves of 95Mg-5ETM powder mixtures during reactive ball milling synthesis; (**b**) the corresponding absorption rates (derivative curves of a); and (**c**) hydrogen sorption curves at 573 K of MgH_2-$ETMH_x$ NCs for different sorption sweeps. (Reproduced from ref. [58]. Copyright 2019 RSC).

Zhou et al. [90] prepared 49 additive-doped MgH_2 samples by ultra-high-energy-high-pressure ball milling, in order to conduct a comprehensive survey on a wide range of additives and corresponding dehydrogenation temperatures of the catalyzed MgH_2. The plot of the Thermogravimetric Analysis (TGA) dehydrogenation temperatures is shown in Figure 8, indicating that the additives containing the IV-B and V-B group elements are the most effective catalysts while the VII-B (Mn), VIII-B (Fe, Co, and Ni) groups show moderate catalytic effects. Besides, Ti and its compounds are more effective compared to those catalysts based on heavier elements (Zr, ZrH_2, ZrO_2, and Ta) in the same periodic group.

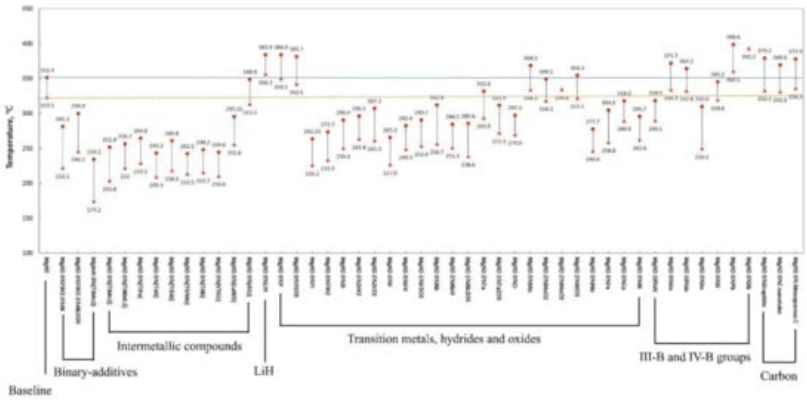

Figure 8. Effect of various additives on dehydrogenation temperatures of MgH_2. (Reprinted with permission from ref. [90]. Copyright 2015 Elsevier).

Cui et al. [91] synthesized micro-sized Mg particles coated with nano-sized TM catalyst, showing that the nano-coating of TM on the Mg/MgH_2 surface is more effective than co-ball-milling of Mg with TMs. The authors also suggested that the catalytic improvement on dehydrogenation kinetics can be ranked as Mg-Ti, Mg-Nb, Mg-Ni, Mg-V, Mg-Co, and Mg-Mo, and the hydrogenation kinetics is in a sequence of Mg-Ni, Mg-Nb, Mg-Ti, Mg-V, Mg-Co, and Mg-Mo.

It has been recognized that early transition metals (ETM) belong to the group of most effective catalysts. Despite some discrepancies in reported data, Ti-based catalysts, involving not only elemental Ti but also Ti hydrides, oxides, halides, and intermetallic compounds have shown great benefits in improving the hydrogen storage properties of MgH_2. In-depth investigations of Ti-based catalysts are also beneficial for understanding the catalysis mechanism for the Mg-H_2 system.

3.2. Catalytic Effects of Ti-Based Compounds

A large number of Ti-based catalysts have been explored for enhancing the hydrogen storage properties of MgH_2. Early attempts using elemental Ti powder to ball-mill with MgH_2 received encouraging results [57]. Soon, researchers found that TiH_2 powder additive is very effective as well. Lu et al. [92] reported exceptional room temperature hydrogenation properties of MgH_2-0.1TiH_2 material prepared by ultra-high-energy-high-pressure (UHEHP) ball milling. Liu et al. [72] studied the effects of two different Ti hydrides ($TiH_{1.971}$ and $TiH_{1.5}$) on the hydrogenation kinetics of Mg. It pointed out an important fact that elemental Ti can easily react with hydrogen to form various Ti hydrides under certain temperatures and hydrogen pressures. During the reverse hydrogen reaction, the following equations can be summarized:

$$Mg + Ti + H_2 \rightarrow Mg + TiH_{1.971} \quad (1)$$

$$Mg + TiH_{1.5} + TiH_{1.971} + H_2 \rightarrow MgH_2 + TiH_{1.5} + TiH_{1.971} \quad (2)$$

$$MgH_2 + TiH_{1.5} + TiH_{1.971} \rightarrow Mg + TiH_{1.5} + TiH_{1.971} + H_2 \quad (3)$$

According to the Mg-Ti phase diagram, neither Ti nor Ti hydrides are immiscible with Mg or MgH_2 phases. Furthermore, no ternary Mg-Ti hydride exists in the phase diagram. However, under a metastable condition, it is possible for Ti to dissolve into Mg and form a solid solution. Ponthieu et al. [93] reported Ti solubility in β-MgD_2 up to 7 at.%, and Mg solubility in TiD_2 up to 8%, which suggested shortened D-diffusion path due to the introduction of TiD_2. An Nuclear Magnetic Resonance (NMR) study of MgD_2/TiD_2 composite found lattice coherent fluorite (fcc) structured TiD_2 and MgD_2, which is expected to be a fast H-diffusion pathway to accelerate the kinetics [94].

Another focus is discovering a novel metastable Mg-Ti-H hydride with a new structure. Kyoi et al. [95] synthesized Mg_7-Ti-H FCC hydride using a high-pressure anvil cell. Asano and Akiba reported the ball-milling synthesis of a series of Hexagonal Closest Packed (HCP), Face-centered Cubic (FCC), and Body-centered Cubic (BCC) Mg_xTi_{100-x} alloys, and Mg-Ti-H FCC hydride phases with chemical formulae of $Mg_{40}Ti_{60}H_{113}$ and $Mg_{29}Ti_{71}H_{57}$. These ternary hydrides had lower stabilities in comparison to MgH_2 and thus show lower desorption temperatures.

TiO_2 was considered an effective catalyst. Wang et al. [75] prepared ball-milled Mg-TiO_2 and showed good hydrogenation and dehydrogenation kinetics. For the past two decades, however, the investigation of oxide catalysts paid more attention to Nb_2O_5, since it seems to be more efficient among transition metal oxides [96]. Actually, doping of TiO_2 would present a similar effect comparing to the Nb_2O_5 catalyst. As suggested by Pukazhselvan et al. [97], TiO_2 can be partially reduced to a lower $3^+/2^+$ state (TiO and Ti_2O_3). The presence of $Mg_xTi_yO_{x+y}$ oxide was also suspected, but no direct support was seen by X-ray Diffraction (XRD) results. More recently, Zhang et al. [98] showed good catalytic activity of carbon-supported nanocrystalline TiO_2 (TiO_2@C). It was reported that the dehydrogenation temperature of MgH_2-10 wt%TiO_2@C can be

lowered to 205 °C and hydrogen uptake took place at room temperature. Berezovets et al. [99] reported that the Mg-5 mol% $Ti_4Fe_2O_x$ was able to absorb hydrogen even at room temperature after hydrogen desorption at 300–350 °C and its cycling stability could be substantially improved by introduction of 3 wt% graphite into the composite.

Ti halides have been reported to offer a positive effect on the kinetics of MgH_2. TM fluorides usually present superior catalytic effects and satisfactory kinetics. Malka et al. [80] reported the catalytic effects of a group of TM fluorides (FeF_2, NiF_2, TiF_3, NbF_5, VF_4, ZrF_4, CrF_2, CuF_2, CeF_3, and YF_3) on the kinetics of MgH_2. The best catalysts for magnesium hydride decomposition were selected to be ZrF_4, TaF_5, NbF_5, VCl_3, and $TiCl_3$. In another investigation by Jin et al. [100], it was suggested that TiF_3 and NbF_5 showed better effects over other TM fluorides. It was found that the hydride, for example, TiH_2, formed after co-milling MgH_2 with the fluorides, with an in situ reaction described as follows:

$$3MgH_2 + 2TiF_3 \rightarrow 3MgF_2 + 2TiH_2 + H_2 \quad (4)$$

Moreover, Wang et al. [101] conducted a comparison study on the elemental Ti, TiO_2, TiN, and TiF_3 catalyzed MgH_2 materials, showing that TiF_3 had the strongest catalytic effect among them.

Ti-based intermetallics as catalysts have been receiving active attention in recent years. Early researchers used TiFe [102], $(Fe_{0.8}Mn_{0.2})Ti$ [103], Ti_2Ni [104], and $TiMn_{1.5}$ [105] additives to improve hydrogen storage properties of MgH_2, showing that all these intermetallics were effective catalysts. Interestingly, some Ti-based intermetallics themselves, including TiFe and $TiMn_{1.5}$, are known as hydrogen storage alloys. Zhou et al. [56] conducted a systematic investigation focusing on a series of Ti-based intermetallic catalysts (i.e., TiAl, Ti3Al, TiNi, TiFe, TiNb, $TiMn_2$, and TiVMn). The results found that $TiMn_2$-doped Mg demonstrated extraordinary hydrogen absorption capability at room temperature and 1-bar hydrogen pressure while its apparent activation energy is 20.59 kJ/mol·H_2. The strong catalytic effect of $TiMn_2$ is also confirmed by another experimental work by El-Eskandarany et al. [106][107] and first principles calculation by Dai et al. [108].

4. Synthetic Approaches

The synthesis methods of Mg-based hydrides have a great impact on their hydrogen storage properties. With expanding research scope of hydrogen storage materials, there are emerging preparation methods in recent years. Many hydrogen storage alloys can be prepared by physical methods, including ball milling [109], induction melting [110], arc melting [111], et cetera. Complex hydrides are usually prepared by chemical methods, such as organic synthesis, hydrothermal method, and solvothermal method [112]. However, conventional high-temperature preparations such as sintering or melting have been largely restricted due to the low melting temperature and high vapor pressure of magnesium [15]. Widely-used methods for Mg-based hydride preparation include ball milling, thin film deposition, and chemical methods.

5. Mechanisms of Catalysis

Understanding the catalysis is critical to improving hydrogen absorption and desorption kinetics for Mg-based systems. Based on the understanding of the hydrogen reaction in the metal-hydrogen system [113], the hydrogenation of metal should go through the following five steps: (1) Physisorption of the H_2 molecule, (2) dissociation of the H_2 molecule, (3) surface penetration of H atoms, (4) diffusion of H atoms in the host lattice, and (5) hydride formation at metal/hydride interface, as shown in Figure 9. For the dehydrogenation reaction, a hydride particle could go through the following steps: (1) Hydride decomposition, (2) diffusion of hydrogen atom, (3) surface penetration, (4) recombination to hydrogen molecule, and (5) desorption to the gas phase. Either hydrogen absorption or desorption should be controlled by a rate-limiting step while other steps are likely in equilibrium.

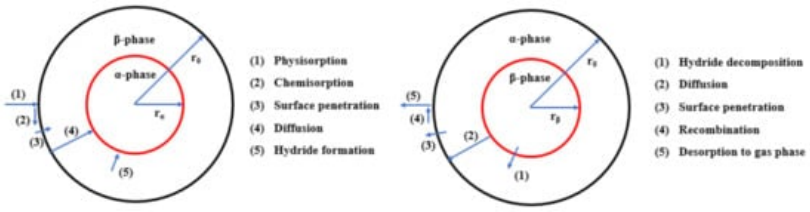

Figure 9. Reaction partial steps for the absorption (**left**) and desorption (**right**) of hydrogen by a spherical metal/hydride powder particle. (Reproduced with permission from ref. [113]. Copyright 1996 Elsevier).

However, the rate-controlling mechanisms in hydrogenation and dehydrogenation may not necessarily be the same. The physisorption of a H_2 molecule on a metal surface needs a very low activation energy, so it is generally not considered a limiting step. The rest of the steps can be rate-limiting which is worthy of discussion. For dehydrogenation, steps 1, 2, and

3 (illustrated in Figure 9) can be considered as possible rate-limiting steps. Note that the hydrogen atoms should diffuse across the metal phase, in which the diffusion coefficient is much higher compared to that in the hydride phase. Moreover, the dehydrogenation has a H_2 recombination step instead of dissociation. The recombination of H atoms into a molecule does not have an energy barrier to overcome [114]. From these aspects, it seems reasonable that the kinetic barrier of dehydrogenation could be lower than that of hydrogenation. However, dehydrogenation is an endothermic reaction whereas hydrogenation is exothermic, which means the hydrogenation of Mg is favored in respect of thermodynamics. These fundamental differences may change the activation barrier and lead to different reaction behaviors.

References

1. Harapan, H.; Mudatsir, M.; Yufika, A.; Nawawi, Y.; Wahyuniati, N.; Anwar, S.; Yusri, F.; Haryanti, N.; Wijayanti, N.P.; Rizal, R.; et al. Hydrogen and fuel cells: Towards a sustainable energy future. Energy Policy 2008, 36, 4356–4362.
2. Felderhoff, M.; Weidenthaler, C.; von Helmolt, R.; Eberle, U. Hydrogen storage: The remaining scientific and technological challenges. Phys. Chem. Chem. Phys. 2007, 9, 2643–2653.
3. Jollibois, M.P. Sur la formule du derive organo-magnesien et sur l'hydrure de magnesium. Compt. Rend. 1912, 155, 353–355.
4. Dymova, T.N.; Sterlyadkina, Z.K.; Safronov, V.G. On the preparation of magnesium hydride. Russ. J. Inorg. Chem. 1961, 6, 763–767.
5. Schlapbach, L.; Züttel, A. Hydrogen-storage materials for mobile applications. Nature 2001, 414, 353–358.
6. Fang, Z.Z.; Zhou, C.; Fan, P.; Udell, K.S.; Bowman, R.C.; Vajo, J.J.; Purewal, J.J.; Kekelia, B. Metal hydrides based high energy density thermal battery. J. Alloys Compd. 2015, 645, S184–S189.
7. Li, J.; Li, B.; Shao, H.; Li, W.; Lin, H. Catalysis and downsizing in Mg-based hydrogen storage materials. Catalysts 2018, 8, 89.
8. Sadhasivam, T.; Kim, H.-T.; Jung, S.; Roh, S.-H.; Park, J.-H.; Jung, H.-Y. Dimensional effects of nanostructured Mg/MgH2 for hydrogen storage applications: A review. Renew. Sustain. Energy Rev. 2017, 72, 523–534.
9. Cheng, F.; Tao, Z.; Liang, J.; Chen, J. Efficient hydrogen storage with the combination of lightweight Mg/MgH2 and nanostructures. Chem. Commun. 2012, 48, 7334–7343.
10. Zhang, X.; Liu, Y.; Hu, J.; Gao, M.; Pan, H. Empowering hydrogen storage performance of MgH2 by nanoengineering and nanocatalysis. Mater. Today Nano 2020, 9, 100064.
11. Aguey-Zinsou, K.-F.; Ares-Fernández, J.-R. Hydrogen in magnesium: New perspectives toward functional stores. Energy Environ. Sci. 2010, 3, 526–543.
12. de Jongh, P.E.; Adelhelm, P. Nanosizing and nanoconfinement: New strategies towards meeting hydrogen storage goals. ChemSusChem 2010, 3, 1332–1348.
13. Shao, H.; He, L.; Lin, H.; Li, H.-W. Progress and Trends in Magnesium-Based Materials for Energy-Storage Research: A Review. Energy Technol. 2018, 6, 445–458.
14. Webb, C.A. A review of catalyst-enhanced magnesium hydride as a hydrogen storage material. J. Phys. Chem. Solids 2015, 84, 96–106.
15. Yartys, V.; Lototskyy, M.; Akiba, E.; Albert, R.; Antonov, V.; Ares, J.; Baricco, M.; Bourgeois, N.; Buckley, C.; Von Colbe, J.B.; et al. Magnesium based materials for hydrogen based energy storage: Past, present and future. Int. J. Hydrogen Energy 2019, 44, 7809–7859.
16. Luo, Q.; Li, J.; Li, B.; Liu, B.; Shao, H.; Li, Q. Kinetics in Mg-based hydrogen storage materials: Enhancement and mechanism. J. Magnes. Alloy. 2019, 7, 58–71.
17. Xie, X.; Chen, M.; Hu, M.; Wang, B.; Yu, R.; Liu, T. Recent advances in magnesium-based hydrogen storage materials with multiple catalysts. Int. J. Hydrogen Energy 2019, 44, 10694–10712.
18. Zhang, Q.; Zang, L.; Huang, Y.; Gao, P.; Jiao, L.; Yuan, H.; Wang, Y. Improved hydrogen storage properties of MgH2 with Ni-based compounds. Int. J. Hydrogen Energy 2017, 42, 24247–24255.
19. Zhang, J.; Li, Z.; Wu, Y.; Guo, X.; Ye, J.; Yuan, B.; Wang, S.; Jiang, L. Recent advances on the thermal destabilization of Mg-based hydrogen storage materials. RSC Adv. 2019, 9, 408–428.
20. Stampfer, J.F.; Holley, C.E.; Suttle, J.F. The magnesium-hydrogen system1-3. J. Am. Chem. Soc. 1960, 82, 3504–3508.

21. Jain, I.; Lal, C.; Jain, A. Hydrogen storage in Mg: A most promising material. Int. J. Hydrogen Energy 2010, 35, 5133–5144.

22. Vajeeston, P.; Ravindran, P.; Hauback, B.C.; Fjellvåg, H.; Kjekshus, A.; Furuseth, S.; Hanfland, M. Structural stability and pressure-induced phase transitions in MgH2. Phys. Rev. B 2006, 73, 224102.

23. Dornheim, M.; Doppiu, S.; Barkhordarian, G.; Boesenberg, U.; Klassen, T.; Gutfleisch, O.; Bormann, R. Hydrogen storage in magnesium-based hydrides and hydride composites. Scr. Mater. 2007, 56, 841–846.

24. Vajeeston, P.; Ravindran, P.; Kjekshus, A.; Fjellvag, H. Pressure-induced structural transitions in MgH2. Phys. Rev. Lett. 2002, 89, 175506.

25. Varin, R.A.; Czujko, T.; Wronski, Z. Particle size, grain size and γ-MgH2 effects on the desorption properties of nanocrystalline commercial magnesium hydride processed by controlled mechanical milling. Nanotechnology 2006, 17, 3856–3865.

26. Felderhoff, M.; Bogdanović, B. High temperature metal hydrides as heat storage materials for solar and related applications. Int. J. Mol. Sci. 2009, 10, 325–344.

27. Satyapal, S.; Petrovic, J.; Read, C.; Thomas, G.; Ordaz, G. The U.S. Department of Energy's National Hydrogen Storage Project: Progress towards meeting hydrogen-powered vehicle requirements. Catal. Today 2007, 120, 246–256.

28. Kohno, T.; Tsuruta, S.; Kanda, M. The hydrogen storage properties of new Mg2Ni alloy. J. Electrochem. Soc. 1996, 143, 198–199.

29. Shao, H.; Wang, Y.; Xu, H.; Li, X. Preparation and hydrogen storage properties of nanostructured Mg2Cu alloy. J. Solid State Chem. 2005, 178, 2211–2217.

30. Bououdina, M.; Guo, Z.X. Comparative study of mechanical alloying of (Mg+ Al) and (Mg+ Al+ Ni) mixtures for hydrogen storage. J. Alloys Compd. 2002, 336, 222–231.

31. Bruzzone, G.; Costa, G.; Ferretti, M.; Olcese, G. Hydrogen storage in Mg51Zn20. Int. J. Hydrogen Energy 1983, 8, 459–461.

32. Chaudhary, A.-L.; Sheppard, D.A.; Paskevicius, M.; Webb, C.J.; Gray, E.M.; Buckley, C.E. Mg2Si Nanoparticle Synthesis for High Pressure Hydrogenation. J. Phys. Chem. C 2014, 118, 1240–1247.

33. Zhou, C.; Fang, Z.Z.; Lu, J.; Zhang, X. Thermodynamic and kinetic destabilization of magnesium hydride using Mg-In solid solution alloys. J. Am. Chem. Soc. 2013, 135, 10982–10985.

34. Si, T.; Cao, Y.; Zhang, Q.; Sun, D.; Ouyang, L.; Zhu, M. Enhanced hydrogen storage properties of a Mg–Ag alloy with solid dissolution of indium: A comparative study. J. Mater. Chem. A 2015, 3, 8581–8589.

35. Spassov, T.; Lyubenova, L.; Köster, U.; Baró, M.D. Mg–Ni–RE nanocrystalline alloys for hydrogen storage. Mater. Sci. Eng. A 2004, 375–377, 794–799.

36. Asano, K.; Enoki, H.; Akiba, E. Effect of Li Addition on Synthesis of Mg-Ti BCC Alloys by means of Ball Milling. Mater. Trans. 2007, 48, 121–126.

37. Asano, K.; Akiba, E. Direct synthesis of Mg–Ti–H FCC hydrides from MgH2 and Ti by means of ball milling. J. Alloys Compd. 2009, 481, L8–L11.

38. Asano, K.; Enoki, H.; Akiba, E. Synthesis of HCP, FCC and BCC structure alloys in the Mg–Ti binary system by means of ball milling. J. Alloys Compd. 2009, 480, 558–563.

39. Asano, K.; Enoki, H.; Akiba, E. Synthesis process of Mg–Ti BCC alloys by means of ball milling. J. Alloys Compd. 2009, 486, 115–123.

40. Vermeulen, P.; van Thiel, E.F.; Notten, P.H. Ternary MgTiX-alloys: A promising route towards low-temperature, high-capacity, hydrogen-storage materials. Chemistry 2007, 13, 9892–9898.

41. Jain, A.; Miyaoka, H.; Ichikawa, T. Destabilization of lithium hydride by the substitution of group 14 elements: A review. Int. J. Hydrogen Energy 2016, 41, 5969–5978.

42. Wagemans, R.W.P.; van Lenthe, J.H.; de Jongh, P.E.; van Dillen, A.J.; de Jong, K.P. Hydrogen storage in magnesium clusters: Quantum chemical study. J. Am. Chem. Soc. 2005, 127, 16675–16680.

43. Zhang, J.; Yan, S.; Qu, H. Stress/strain effects on thermodynamic properties of magnesium hydride: A brief review. Int. J. Hydrogen Energy 2017, 42, 16603–16610.

44. Berube, V.; Chen, G.; Dresselhaus, M. Impact of nanostructuring on the enthalpy of formation of metal hydrides. Int. J. Hydrogen Energy 2008, 33, 4122–4131.

45. Zhu, M.; Lu, Y.; Ouyang, L.; Wang, H. Thermodynamic Tuning of Mg-Based Hydrogen Storage Alloys: A Review. Materials 2013, 6, 4654–4674.

46. Bououdina, M.; Grant, D.; Walker, G. Review on hydrogen absorbing materials—structure, microstructure, and thermodynamic properties. Int. J. Hydrogen Energy 2006, 31, 177–182.

47. Sun, Y.; Shen, C.; Lai, Q.; Liu, W.; Wang, D.-W.; Aguey-Zinsou, K.-F. Tailoring magnesium based materials for hydrogen storage through synthesis: Current state of the art. Energy Storage Mater. 2018, 10, 168–198.

48. Pozzo, M.; Alfè, D. Hydrogen dissociation and diffusion on transition metal (=Ti, Zr, V, Fe, Ru, Co, Rh, Ni, Pd, Cu, Ag)-doped Mg, 0001, surfaces. Int. J. Hydrogen Energy 2009, 34, 1922–1930.

49. Pozzo, M.; Alfe, D.; Amieiro, A.; French, S.; Pratt, A. Hydrogen dissociation and diffusion on Ni- and Ti-doped Mg, 0001, surfaces. J. Chem. Phys. 2008, 128, 094703.

50. Spatz, P.; Aebischer, H.A.; Krozer, A.; Schlapbach, L. The Diffusion of H in Mg and the Nucleation and Growth of MgH2 in Thin Films*. Z. Phys. Chem. 1993, 181, 393–397.

51. Zhou, C. A Study of Advanced Magnesium-Based Hydride and Development of a Metal Hydride Thermal Battery System. Ph.D. Thesis, The University of Utah, Salt Lake City, UT, USA, 2015.

52. Jain, A.; Agarwal, S.; Ichikawa, T. Catalytic tuning of sorption kinetics of lightweight hydrides: A review of the materials and mechanism. Catalysts 2018, 8, 651.

53. Pasquini, L.; Callini, E.; Brighi, M.; Boscherini, F.; Montone, A.; Jensen, T.R.; Maurizio, C.; Antisari, M.V.; Bonetti, E. Magnesium nanoparticles with transition metal decoration for hydrogen storage. J. Nanopart. Res. 2011, 13, 5727–5737.

54. Vincent, S.; Lang, J.; Huot, J. Addition of catalysts to magnesium hydride by means of cold rolling. J. Alloys Compd. 2012, 512, 290–295.

55. Ma, L.-P.; Wang, P.; Kang, X.-D.; Cheng, H.-M. Preliminary investigation on the catalytic mechanism of TiF3 additive in MgH2–TiF3 H-storage system. J. Mater. Res. 2011, 22, 1779–1786.

56. Zhou, C.; Fang, Z.Z.; Ren, C.; Li, J.; Lu, J. Effect of Ti Intermetallic catalysts on hydrogen storage properties of magnesium hydride. J. Phys. Chem. C 2013, 117, 12973–12980.

57. Liang, G.; Huot, J.; Boily, S.; Neste, A.V.; Schulz, R. Catalytic effect of transition metals on hydrogen sorption in nanocrystalline ball milled MgH–Tm (Tm = Ti, V, Mn, Fe and Ni). J. Alloys Compd. 1999, 292, 247–252.

58. Rizo-Acosta, P.; Cuevas, F.; Latroche, M. Hydrides of early transition metals as catalysts and grain growth inhibitors for enhanced reversible hydrogen storage in nanostructured magnesium. J. Mater. Chem. A 2019, 7, 23064–23075.

59. Choi, Y.J.; Choi, J.W.; Sohn, H.Y.; Ryu, T.; Hwang, K.S.; Fang, Z.Z. Chemical vapor synthesis of Mg–Ti nanopowder mixture as a hydrogen storage material. Int. J. Hydrogen Energy 2009, 34, 7700–7706.

60. Patelli, N.; Migliori, A.; Pasquini, L. Reversible metal-hydride transformation in Mg-Ti-H nanoparticles at remarkably low temperatures. ChemPhysChem 2019, 20, 1325–1333.

61. Choi, E.; Song, M.Y. Hydriding and dehydriding features of a titanium-added magnesium hydride composite, materials. Science 2020, 26, 199–204.

62. Lotoskyy, M.; Denys, R.; Yartys, V.A.; Eriksen, J.; Goh, J.; Nyamsi, S.N.; Sita, C.; Cummings, F. An outstanding effect of graphite in nano-MgH2-TiH2 on hydrogen storage performance dagger. J. Mater. Chem. A 2018, 6, 10740–10754.

63. Croston, D.; Grant, D.; Walker, G. The catalytic effect of titanium oxide based additives on the dehydrogenation and hydrogenation of milled MgH2. J. Alloys Compd. 2010, 492, 251–258.

64. Cui, J.; Wang, H.; Liu, J.; Ouyang, L.; Zhang, Q.; Sun, D.; Yao, X.; Zhu, M. Remarkable enhancement in dehydrogenation of MgH2 by a nano-coating of multi-valence Ti-based catalysts. J. Mater. Chem. A 2013, 492, 251–258.

65. Calizzi, M.; Venturi, F.; Ponthieu, M.; Cuevas, F.; Morandi, V.; Perkisas, T.; Bals, S.; Pasquini, L. Gas-phase synthesis of Mg–Ti nanoparticles for solid-state hydrogen storage. Phys. Chem. Chem. Phys. 2016, 18, 141–148.

66. Lu, C.; Zou, J.; Shi, X.; Zeng, X.; Ding, W. Synthesis and hydrogen storage properties of core–shell structured binary Ti and ternary Ni composites. Int. J. Hydrogen Energy 2017, 42, 2239–2247.

67. Choi, Y.J.; Lu, J.; Sohn, H.Y.; Fang, Z.Z.; Rönnebro, E. Effect of milling parameters on the dehydrogenation properties of the Mg−Ti−H system. J. Phys. Chem. C 2009, 113, 19344–19350.

68. Choi, Y.J.; Lu, J.; Sohn, H.Y.; Fang, Z.Z. Hydrogen storage properties of the Mg–Ti–H system prepared by high-energy–high-pressure reactive milling. J. Power Sources 2008, 180, 491–497.

69. Lu, J.; Choi, Y.J.; Fang, Z.Z.; Sohn, H.Y.; Rönnebro, E. Hydrogenation of Nanocrystalline Mg at Room Temperature in the Presence of TiH2. J. Am. Chem. Soc. 2010, 132, 6616–6617.

70. Li, J.; Zhou, C.; Fang, Z.Z.; Bowman, R.C., Jr.; Lu, J.; Ren, C. Isothermal hydrogenation kinetics of ball-milled nano-catalyzed magnesium hydride. Materialia 2019, 5, 100227.

71. Li, J.; Fan, P.; Fang, Z.Z.; Zhou, C. Kinetics of isothermal hydrogenation of magnesium with TiH2 additive. Int. J. Hydrogen Energy 2014, 39, 7373–7381.

72. Liu, T.; Chen, C.; Wang, F.; Li, X. Enhanced hydrogen storage properties of magnesium by the synergic catalytic effect of TiH1.971 and TiH1.5 nanoparticles at room temperature. J. Power Sources 2014, 267, 69–77.

73. Manivasagam, T.G.; Magusin, P.C.M.M.; Iliksu, M.; Notten, P.H.L. Influence of Nickel and Silicon Addition on the Deuterium Siting and Mobility in fcc Mg–Ti Hydride Studied with2H MAS NMR. J. Phys. Chem. C 2014, 118, 10606–10615.

74. Oelerich, W.; Klassen, T.; Bormann, R. Mg-based hydrogen storage materials with improved hydrogen sorption. Mater. Trans. 2001, 42, 1588–1592.

75. Wang, P.; Wang, A.; Zhang, H.; Ding, B.; Hu, Z. Hydrogenation characteristics of Mg–TiO (rutile) composite. J. Alloys Compd. 2000, 313, 218–223.

76. Chen, M.; Xiao, X.; Zhang, M.; Liu, M.; Huang, X.; Zheng, J.; Zhang, Y.; Jiang, L.; Chen, L. Excellent synergistic catalytic mechanism of in-situ formed nanosized Mg2Ni and multiple valence titanium for improved hydrogen desorption properties of magnesium hydride. Int. J. Hydrogen Energy 2019, 44, 1750–1759.

77. Jangir, M.; Gattia, D.M.; Peter, A.; Jain, I.P. Effect of Ti-Additives on Hydrogenation/Dehydrogenation Properties of MgH2. In Proceedings of the 15th International Conference on Concentrator Photovoltaic Systems (CPV-15), Fes, Marocco, 25–27 March 2019; AIP Publishing: College Park, MD, USA, 2019; Volume 2145, p. 020006.

78. Jain, A.; Agarwal, S.; Kumar, S.; Yamaguchi, S.; Miyaoka, H.; Kojima, Y.; Ichikawa, T. How does TiF4 affect the decomposition of MgH2 and its complex variants?—An XPS investigation. J. Mater. Chem. A 2017, 5, 15543–15551.

79. Jangir, M.; Jain, A.; Yamaguchi, S.; Ichikawa, T.; Lal, C.; Jain, I. Catalytic effect of TiF4 in improving hydrogen storage properties of MgH2. Int. J. Hydrogen Energy 2016, 41, 14178–14183.

80. Malka, I.; Czujko, T.; Bystrzycki, J. Catalytic effect of halide additives ball milled with magnesium hydride. Int. J. Hydrogen Energy 2010, 35, 1706–1712.

81. Kalisvaart, W.; Harrower, C.; Haagsma, J.; Zahiri, B.; Luber, E.; Ophus, C.; Poirier, E.; Fritzsche, H.; Mitlin, D. Hydrogen storage in binary and ternary Mg-based alloys: A comprehensive experimental study. Int. J. Hydrogen Energy 2010, 35, 2091–2103.

82. Zahiri, B.; Amirkhiz, B.S.; Mitlin, D. Hydrogen storage cycling of MgH2 thin film nanocomposites catalyzed by bimetallic Cr Ti. Appl. Phys. Lett. 2010, 97, 083106.

83. Yao, X.; Wu, C.; Du, A.; Zou, J.; Zhu, Z.; Wang, P.; Cheng, H.; Smith, S.C.; Lu, G. Metallic and carbon nanotube-catalyzed coupling of hydrogenation in magnesium. J. Am. Chem. Soc. 2007, 129, 15650–15654.

84. Liu, T.; Chen, C.; Wang, H.; Wu, Y. Enhanced hydrogen storage properties of Mg–Ti–V nanocomposite at moderate temperatures. J. Phys. Chem. C 2014, 118, 22419–22425.

85. Berlouis, L.E.A.; Honnor, P.; Hall, P.J.; Morris, S.; Dodd, S.B. An investigation of the effect of Ti, Pd and Zr on the dehydriding kinetics of MgH2. J. Mater. Sci. 2006, 41, 6403–6408.

86. Chen, C.; Wang, J.; Wang, H.; Liu, T.; Xu, L.; Li, X.I. Improved kinetics of nanoparticle-decorated Mg-Ti-Zr nanocomposite for hydrogen storage at moderate temperatures. Mater. Chem. Phys. 2018, 206, 21–28.

87. Huang, X.; Xiao, X.; Wang, X.; Wang, C.; Fan, X.; Tang, Z.; Wang, C.; Wang, Q.; Chen, L. Synergistic catalytic activity of porous rod-like TMTiO3 (TM = Ni and Co) for reversible hydrogen storage of magnesium hydride. J. Phys. Chem. C 2018, 122, 27973–27982.

88. Daryani, M.; Simchi, A.; Sadati, M.; Hosseini, H.M.; Targholizadeh, H.; Khakbiz, M. Effects of Ti-based catalysts on hydrogen desorption kinetics of nanostructured magnesium hydride. Int. J. Hydrogen Energy 2014, 39, 21007–21014.

89. Chen, M.; Xiao, X.; Zhang, M.; Zheng, J.; Liu, M.; Wang, X.; Jiang, L.; Chen, L. Highly dispersed metal nanoparticles on TiO2 acted as nano redox reactor and its synergistic catalysis on the hydrogen storage properties of magnesium hydride. Int. J. Hydrogen Energy 2019, 44, 15100–15109.

90. Zhou, C.; Fang, Z.Z.; Sun, P. An experimental survey of additives for improving dehydrogenation properties of magnesium hydride. J. Power Sources 2015, 278, 38–42.

91. Cui, J.; Liu, J.; Wang, H.; Ouyang, L.; Sun, D.; Zhu, M.; Yao, X. Mg–TM (TM: Ti, Nb, V, Co, Mo or Ni) core–shell like nanostructures: Synthesis, hydrogen storage performance and catalytic mechanism. J. Mater. Chem. A 2014, 2, 9645–9655.

92. Lu, J.; Choi, Y.J.; Fang, Z.Z.; Sohn, H.Y.; Rönnebro, E. Hydrogen storage properties of nanosized MgH2-0.1TiH2 prepared by ultrahigh-energy-high-pressure milling. J. Am. Chem. Soc. 2009, 131, 15843–15852.
93. Ponthieu, M.; Cuevas, F.; Fernández, J.F.; Laversenne, L.; Porcher, F.; Latroche, M. Structural properties and reversible deuterium loading of MgD2–TiD2 nanocomposites. J. Phys. Chem. C 2013, 117, 18851–18862.
94. Emery, S.B.; Sorte, E.G.; Bowman, R.C.; Fang, Z.Z.; Ren, C.; Majzoub, E.H.; Conradi, M.S. Detection of fluorite-structured MgD2/TiD2: Deuterium NMR. J. Phys. Chem. 2015, 119, 7656–7661.
95. Kyoi, D.; Sato, T.; Rönnebro, E.; Kitamura, N.; Ueda, A.; Ito, M.; Katsuyama, S.; Hara, S.; Noréus, D.; Sakai, T. A new ternary magnesium–titanium hydride Mg7TiHx with hydrogen desorption properties better than both binary magnesium and titanium hydrides. J. Alloys Compd. 2004, 372, 213–217.
96. Oelerich, W.; Klassen, T.; Bormann, R. Metal oxides as catalysts for improved hydrogen sorption in nanocrystalline Mg-based materials. J. Alloys Compd. 2001, 315, 237–242.
97. Pukazhselvan, D.; Nasani, N.; Correia, P.; Carbó-Argibay, E.; Otero-Irurueta, G.; Stroppa, D.G.; Fagg, D.P. Evolution of reduced Ti containing phase(s) in MgH2/TiO2 system and its effect on the hydrogen storage behavior of MgH2. J. Power Sources 2017, 362, 174–183.
98. Zhang, M.; Xiao, X.; Luo, B.; Liu, M.; Chen, M.; Chen, L. Superior de/hydrogenation performances of MgH2 catalyzed by 3D flower-like TiO2@C nanostructures. J. Energy Chem. 2020, 46, 191–198.
99. Berezovets, V.; Denys, R.; Zavaliy, I.; Kosarchyn, Y. Effect of Ti-based nanosized additives on the hydrogen storage properties of MgH2. Int. J. Hydrogen Energy 2021.
100. Jin, S.-A.; Shim, J.-H.; Cho, Y.W.; Yi, K.-W. Dehydrogenation and hydrogenation characteristics of MgH2 with transition metal fluorides. J. Power Sources 2007, 172, 859–862.
101. Wang, Y.; Zhang, Q.; Wang, Y.; Jiao, L.; Yuan, H. Catalytic effects of different Ti-based materials on dehydrogenation performances of MgH2. J. Alloys Compd. 2015, 645, S509–S512.
102. Guoxian, L.; Erde, W.; Shoushi, F. Hydrogen absorption and desorption characteristics of mechanically milled Mg-35 wt%FeTi1.2 powders. J. Alloys Compd. 1995, 223, 111–114.
103. Reule, H.; Hirscher, M.; Weißhardt, A.; Kronmüller, H. Hydrogen desorption properties of mechanically alloyed MgH2 composite materials. J. Alloys Compd. 2000, 305, 246–252.
104. Cui, N.; Luan, B.; Zhao, H.; Liu, H.K.; Dou, S.X. Synthesis and electrode characteristics of the new composite alloys Mg2Ni-xwt%Ti2Ni. J. Alloys Compd. 1996, 240, 229–234.
105. Hu, Y.; Zhang, H.; Wang, A.; Ding, B.; Hu, Z. Preparation and hydriding/dehydriding properties of mechanically milled Mg–30 wt% TiMn1.5 composite. J. Alloys Compd. 2003, 354, 296–302.
106. El-Eskandarany, M.S.; Shaban, E.; Aldakheel, F.; Alkandary, A.; Behbehani, M.; Al-Saidi, M. Synthetic nanocomposite MgH2/5 wt. % TiMn2 powders for solid-hydrogen storage tank integrated with PEM fuel cell. Sci. Rep. 2017, 7, 13296.
107. El-Eskandarany, M.S.; Al-Ajmi, F.; Banyan, M.; Al-Duweesh, A. Synergetic effect of reactive ball milling and cold pressing on enhancing the hydrogen storage behavior of nanocomposite MgH2/10 wt% TiMn2 binary system. Int. J. Hydrogen Energy 2019, 44, 26428–26443.
108. Dai, J.H.; Jiang, X.W.; Song, Y. Stability and hydrogen adsorption properties of Mg/TiMn2 interface by first principles calculation. Surf. Sci. 2016, 653, 22–26.
109. Hanada, N.; Ichikawa, T.; Fujii, H. Catalytic effect of Ni nano-particle and Nb oxide on H-desorption properties in MgH2 prepared by ball milling. J. Alloys Compd. 2005, 404–406, 716–719.
110. Pourabdoli, M.; Raygan, S.; Abdizadeh, H.; Uner, D. A comparative study for synthesis methods of nano-structured (9Ni–2Mg–Y) alloy catalysts and effect of the produced alloy on hydrogen desorption properties of MgH2. Int. J. Hydrogen Energy 2013, 38, 16090–16097.
111. Elanski, D.; Lim, J.-W.; Mimura, K.; Isshiki, M. Thermodynamic estimation of hydride formation during hydrogen plasma arc melting. J. Alloys Compd. 2007, 439, 210–214.
112. Elanski, D.; Lim, J.-W.; Mimura, K.; Isshiki, M. Complex hydrides for energy storage, conversion, and utilization. Adv. Mater. 2019, 31, e1902757.
113. Martin, M.; Gommel, C.; Borkhart, C.; Fromm, E. Absorption and desorption kinetics of hydrogen storage alloys. J. Alloys Compd. 1996, 238, 193–201.
114. Hollenbach, D.; Salpeter, E.E. Surface recombination of hydrogen molecules. Astrophys. J. 1971, 163, 155.